23rd ABCM International Congress of Mechanical Engineering
December 6-11, 2015, Rio de Janeiro, RJ, Brazil

EXPERIMENTAL EVALUATION OF THE MULTI-POINT SOURCE MODEL FOR PREDICTING RADIATIVE HEAT FLUX EMITTED BY METHANE DIFFUSION FLAMES

Isaías Mortari Machado
Rodrigo Brenner Miguel
Nattan Roberto Caetano
Francis Henrique Ramos França
Fernando Marcelo Pereira
Federal University of rio Grande do Sul – Rua Sarmento Leite, 425 – Porto Alegre - RS
imortarim@gmail.com
rodrigo.miguel@ufrgs.br
nattan@ufrgs.br
frfranca@mecanica.ufrgs.br
fernando@mecanica.ufrgs.br

Paulo Roberto Pagot
PETROBRAS–Petróleo Brasileiro S.A. CENPES, Av. Horácio Macedo, 950 – Rio de Janeiro – RJ.
pagot@petrobras.com.br

Abstract. *The purpose of this paper is to present an experimental study for obtaining of the weighting factors for the weighted multi-point source model (WMPS) used to predict the radiative heat flux from diffusion flames. The WMPS model assumes that the radiative heat flux incident on a receptor is the result of several source points located along the flame axis, each point being associated with a weighting factor. The weighting factors are obtained from measurements of the radiative heat flux from the flame with a radiometer. The view angle of the radiometer is reduced by a slit. The radiative heat fluxes obtained from the model are compared with the distribution of radiative heat fluxes measured for the flames at distances smaller than the visible flame length. It is shown that the use of these weighting factors results in good agreement with the heat flux measured along the flame axis.*

Keywords: *Radiative heat transfer, multi-point source model, diffusion flames.*

1. INTRODUCTION

The modeling of radiative heat transfer in combustion processes is a challenging task. The radiant heat losses are coupled with the combustion mechanisms, influencing directly the burning rates and species formation. The knowledge of the radiative characteristics of flames is of paramount importance for industrial applications such as engines, furnaces, burners and flares. Specifically for flares, the prediction of the radiant heat flux near the flame and the distribution of heat flux along the flame are necessary to evaluate safety conditions, to assess potential risk scenarios and to protect equipment and structures.

The heat exchanged by radiation in hydrocarbon diffusion flames is mainly due to spectral bands emission from water vapor and carbon dioxide and to continuous spectral emission from soot particles. The presence of soot increases substantially the heat transfer by radiation (Nathan *et al*. 2012) and is responsible for the yellow luminosity of the visible flame.

Simplified models are useful for several engineering applications. Some of these models consider that the flame can be represented by source points. The simplest model is the single point source model (SPS), where the source of radiation in the flame is represented by one point located at the half visible flame length. This model is used in the API standard for flaring systems (ANSI/API STANDARD 521, 2008) and in several works about the radiative characteristics of flames (Turns and Myhr, 1991; Markstein, 1977; Becker and Liang, 1982). This model is widely used to predict the radiative heat flux in the far field regions, which is represented by distances up from two visible flame lengths, but fails in the near field region. Models like the weighted multi-point source model (WMPS) (Hankinson and Lowesmith, 2012) are of interest because they keep the simplicity of the SPS model but are able to predict the radiative heat flux in the near field regions (distances up to two visible flame lengths).

The model considered must be able to predict the effects of cross winds and fuel dilution. Fuel dilution became relevant because mixtures of hydrocarbon with diluents are frequently found in alternative fuel sources like biogas. For applications like flaring systems in off-shore platforms in the Brazilian pre-salt the fuel dilution effects gets special relevance, because the natural gas extracted from these oil fields presents up to 50% of carbon dioxide in volume. A fuel composed of methane and carbon dioxide, as compared with pure methane, has a lower calorific content, lower flame speed, lower flame temperature and higher molar mass. The combustion products produced have a higher concentration of CO_2, which is a participating gas, that is emits and absorbs radiation, affecting the heat transfer with the surroundings. Another effect of fuel dilution is the inhibition of soot formation (Mishra and Kumar, 2010; Turns *et al*., 1991; Axelbaum *et al*., 1988), caused by the decrease in flame temperature and the decrease in soot precursors concentration.

The present works aims to verify the capability of the WMPS model to predict the radiative heat flux emitted from flames in the near field. To verify this capability, two independent measurements are made in natural gas flames with different dilutions with CO_2. The first measurements are made to provide the radiative heat fluxes at a fixed distance from the flame axis, the second measurements are made closer to the flame axis with the view angle of the sensor restricted, aiming at observing a small region of the flame. These last measurements are used to generate the weighting factors of the model.

2. WEIGHTED MULTI-POINT SOURCE MODEL

The WMPS model was proposed by Hankinson and Lowesmith (2012), based on the multi-ray model studied by Sivathanu and Gore (1993). This model assumes that the flame can be represented by a finite number of point sources distributed along the flame axis (Fig. 1a). The radiative heat flux (q^{WMPS}) observed at a defined location is given by Eq. 1, which the sum of the effect of each point source weighted by a weighting factor (w_j).

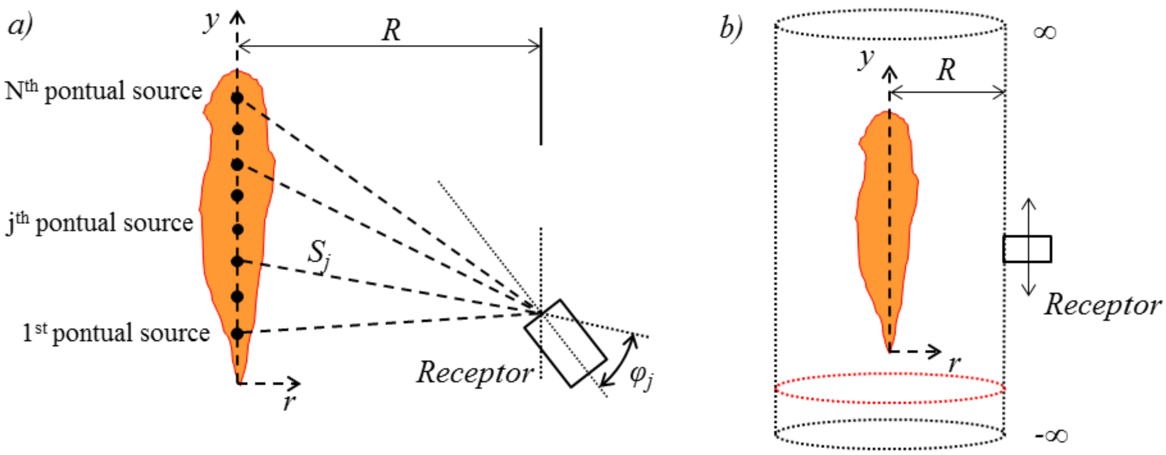

Figure 1. a) Weighted multi-point source model; b) Method used to evaluate the radiant fraction

$$q^{WMPS} = \sum_{j=1}^{N} w_j \frac{X_r Q_f \tau_{S_j}}{4\pi S_j^2} \cos\varphi_j \tag{1}$$

where X_r is the radiant fraction, which is defined as the rate between the radiated heat (Q_r) and the total heat released of the flame (Q_f), τ_{Sj} is the transmittance evaluated at distance S_j between the receptor and the source and φ_j is the angle between the normal axis of the surface of the receptor and the direction of S_j. The values for transmittance at the distances present in this work (less than 5 meters) can be considered unit.

The weighting factor proposed by Hankinson and Lowesmith (2012) are situated in the visible flame length and are defined by two linear equations, the first start in zero at position $y = 0$, the maximum value at the position $y = 0.75\ L_f$. The second equation starts with the maximum value at position $y = 0.75\ L_f$ and go to zero at the position $y = L_f$. The sum of the weighting factors must be the unit. They proposed also that the flame must be approximated by at least 20 point sources.

The value for radiated fraction (X_r) can be obtained experimentally by the integration of the radiative heat fluxes measured (q_i'') along the flame axis (Fig. 1b). X_r is calculated as

$$X_r = \frac{Q_r}{Q_f} = \frac{\int_{-\infty}^{\infty} q_i'' \, 2\pi R dy}{Q_f \tau_S} \approx \sum_{i=1}^{N} \frac{q_i'' \, 2\pi R \Delta y}{\dot{m}_{fuel} LHV} \tag{2}$$

where Δy is the discreet height where the radiative heat flux is measured. The values of X_r for methane flames vary from 0.08 to 0.20 (Becker and Liang, 1982; Turns and Myhr, 1991). In experimental studies, a practical limit for the radiation sensor displacement can be assumed as where the heat flux measured is smaller than two times the background radiation (Machado, 2015).

3. METHODS AND EXPERIMENTAL SETUP

Figure 2a shows a diagram of the experimental apparatus and Fig. 2b shows the burner used. The burner is composed by an injector 235 mm long with 7.4 mm inner diameter and a rectifier camera 71 mm long where the gas mixture flows thru glass beads and screens. The burner is attached at the structure in a fixed position. The different vertical positions are obtained by displacing the sensor along the vertical axis. The flow rates are controlled and measured with mass flow rates controllers Bronkhorst EL200 series. The positioning is verified with a graduated scale.

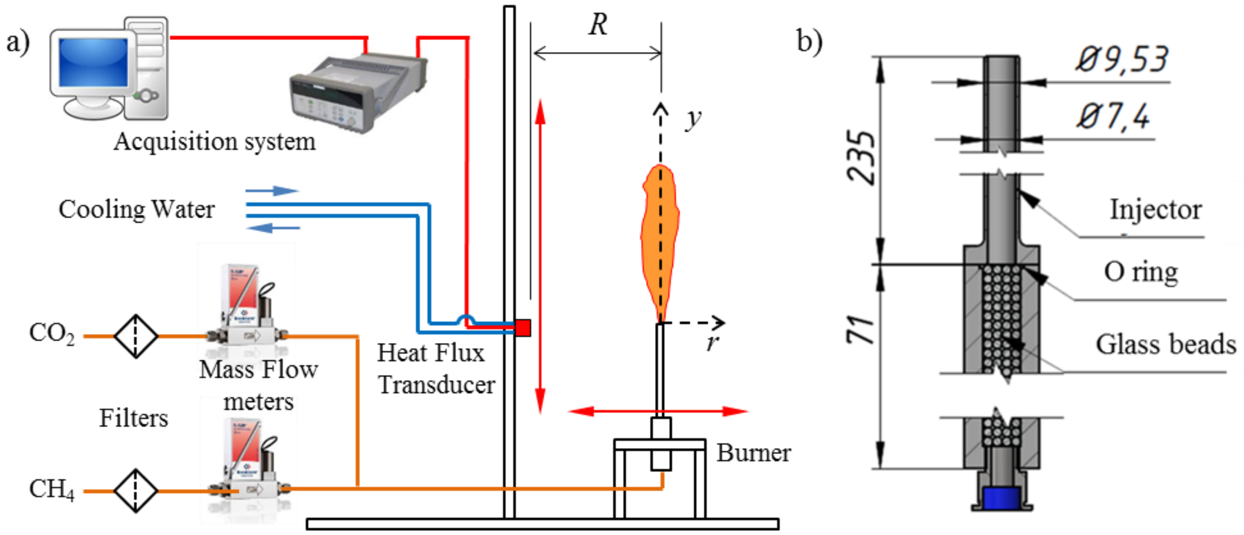

Figure 2. a) Diagram of the experimental apparatus. b) Burner used in the experiments (dimensions in millimeters)

The sensor used is a MEDTHERM heat flux transducer model 64-0.5-20/ZnSeW-1C-150. This transducer is a Schmidt-Boelter thermopile with a ZnSe window which has a flat spectral transmissivity of 70% for a wavelength interval form 0.7 µm to 17 µm. The view angle of the sensor is 150° and its response time is 300 ms. The heat flux transducer is cooled with water at 298 K. The signal acquisition is made with a 34970A Agilent Data Logger.

The radiative heat flux is given by the signal multiplied by the calibration constant of the sensor, which is factory calibrated. The uncertainty associated with the signal is calculated as

$$U_{0.95} = \left[(B_{Xi})^2 + (tS_{Xi})^2 \right]^{0.5} \quad (3)$$

where B_{Xi} is the uncertainty associated with the measurement system, given by the root square sum (RSS) of the uncertainties from each source of error, that are the accuracy of the transducer (3% of the signal), the repeatability of the transducer (0.5% of the signal), the uncertainty of the data logger (0.0030% of the signal) and the uncertainty of the data logger associated with the measurement range (0.0035% of the range for the 100 mV range). t is the Student's t for 95% of confidence and S_{Xi} is the variance of the acquired signal. For each measurement position 50 samples (400 ms between samples) were collected and averaged.

For each position, the signal for the radiative heat flux is given by the difference between the signal obtained with the transducer exposed to the flame and the background signal and the final uncertainty is given by the RSS of the this two uncertainties.

The radiant fraction is calculated with the forth term of Eq. 2 and its uncertainty is calculated, following Moffat (1988), as

$$U_{Xr} = \left[\left(\frac{\partial X_r}{\partial q_i''} \delta q_i'' \right)^2 + \left(\frac{\partial X_r}{\partial R} \delta R \right)^2 + \left(\frac{\partial X_r}{\partial \Delta y} \delta \Delta y \right)^2 + \left(\frac{\partial X_r}{\partial V_0} \delta V_0 \right)^2 \right]^{0.5} \quad (4)$$

where $\delta q_i''$ is the uncertainty associated with heat flux measured at each position (RSS of the uncertainty of the signal from the flame and the background), δR is the uncertainty associated with the radial positioning (assumed ± 2 mm), $\delta \Delta y$ is the uncertainty of Δy (which, in fact, accounts for the uncertainty of the total area for the numerical integration of the radiative heat flux) and δV_0 is the uncertainty associated with the mass flow rate of methane.

For each flame, two independent measurements were made. In the first the distribution of the radiative heat fluxes and the radiated fraction were obtained, in the second, the weighting factors for the WMPS model are obtained. To obtain the w_j, the view angle of the transducer was vertically restricted, reducing the height of the flame viewed by the sensor. For each position along the flame axis it is measured a signal for the radiated heat flux (I_j). The weighting factors for each position are given by

$$w_j = \frac{I_j}{\sum_{j=1}^{N} I_j} \tag{5}$$

The distribution of radiative heat fluxes were obtained at the radial position (R) 199 mm. The visible flame lengths (L_f) were evaluated from the average of 150 sequential images of each flame (obtained at 30 Hz), where L_f is taken as the maximum length observed. This paper studies a set of flames of natural gas (NG) diluted with carbon dioxide which the parameters are presented in Table 1. These parameters were specified aiming to observe the effect of CO_2 dilution in flames with the same heat released and in flames with the same mixture inject velocity. The natural gas used is composed by 90.8% of methane, 6.1% of ethane, 1.2% of propane and 1.9% of higher hydrocarbons and inert gases (GASNET,2013).

Table 1. Parameters of the studied flames.

Flame code		3.00-0.00	3.00-0.75	3.00-2.00	2.40-0.60	1.80-1.20
Mass flow rate (*l/min*)[a]	NG	3.00	3.00	3.00	2.40	1.80
	CO_2	0.00	0.75	2.00	0.60	1.20
	total	3.00	3.75	5.00	3.00	3.00
Dilution (%)		0	20	40	20	40
Heat released (kW)		1.663	1.663	1.663	1.331	0.998
Re[b]		515	775	1205	620	723

a) measured in standard condition: 273.15 K and 1 atm.
b) The viscosity of the fuel mixture was evaluated by a molecular average.

4. RESULTS AND DISCUSSIONS

The characteristics of the flames studied are presented in Table 2 and a representative image of each flame is presented in Fig. 3. The characteristic residence time (τ_G) is based on the definition of Turns and Myhr (1991).

Table 2. Measured characteristics of the studied flames.

Flame	3.00-0.00	3.00-0.75	3.00-2.00	2.40-0.60	1.80-1.20
X_r	0.1782	0.1656	0.1561	0.1615	0.1546
U_{X_r}	0.0091	0.0112	0.0106	0.0099	0.0069
L_f (mm)	396	391	407	348	288
τ_G (ms)	136	129	140	113	82

It is observed that the radiated fraction of the flames is reduced with the increase of dilution. This can be explained by the reduction in the flame temperature and the inhibition of soot formation, which is an important specie for thermal radiation emission in flames. The inhibition of soot formation is evidenced by the reduction in the yellow luminosity of the flame and the increase in the soot free length fraction, as observed in Fig. 3. The visible flame length remains almost constant for the flames with the same heat release and is reduced with the increasing in dilution for the flames with the same mixture flow rate. This occurs because in constant flow rate flames the amount of fuel that really burns is reduced with the dilution.

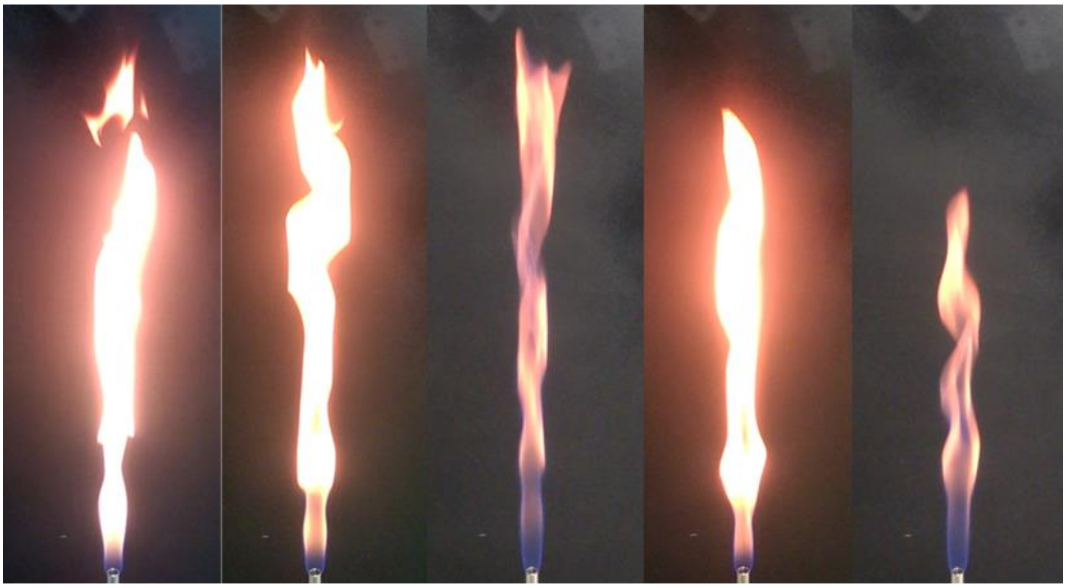

Figure 3. Representative image of the studied flames

Figure 4 presents the normalized weighting factors proposed by Hankinson and Lowesmith (2012) and the experimentally obtained in this work. They are normalized by the maximum value of w_j of each flame. This is necessary because the values of w_j are dependent of the number of factors evaluated. For the use in the model, they must be divided by the sum of the factors, since the sum of the w_j must be the unity.

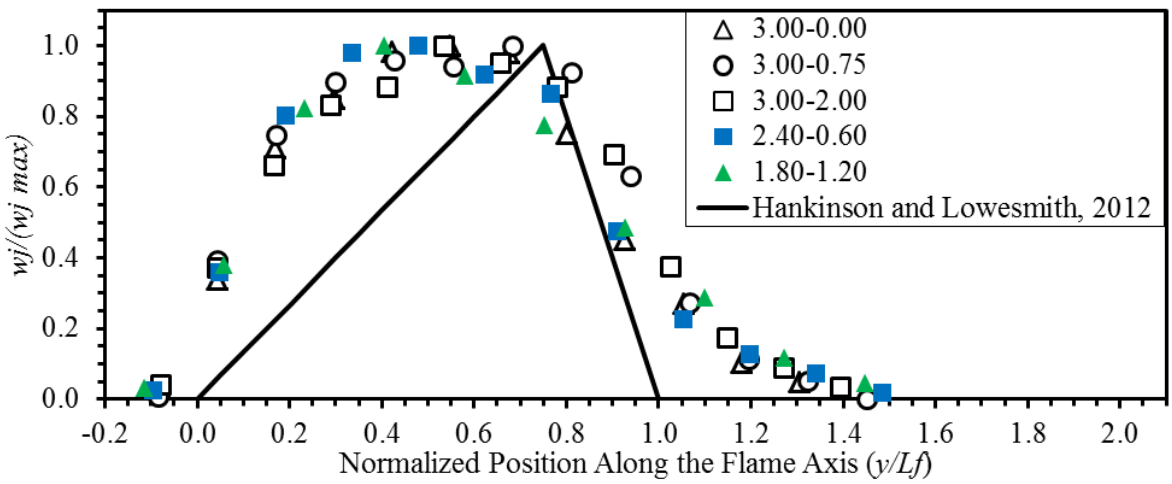

Figure 4. Comparison of the measured weighting factors with the factors from Hankinson and Lowesmith (2012)

The different fuel dilutions produced flames with similar distribution of w_j measured and this distribution is different of that present in the literature. The differences are the presence of sources beyond the flame top (L_f=1) and the existence of a region of maximum emission from 0.3 L_f to 0.75 L_f instead a peak on 0.75 L_f.

Figure 5 presents the comparison between the distributions of radiative heat fluxes measured, and the obtained with the WMPS model using the experimental weighting factors (WMPSE) and the weighting factors from Hankinson and Lowesmith (2012) (WMPSL) for the flame 3.00-0.00. For the WMPSL were considered 21 sources along the visible flame length, for the WMPSE were used 13 sources distributed as is presented in Fig. 4.

It is observed that both distributions of weighting factor give good agreement with the experimental data for positions beyond 1.1 L_f. The WMPSL underestimates the radiative heat fluxes for position up to 0.4 L_f and overestimates for the region between 0.5 L_f and 0.8 L_f. The R^2 obtained for this curve is 0.976. The WMPSE underestimates the radiative heat fluxes from 0.4 L_f to 1 L_f, but for position below 0.4 L_f, the fluxes obtained stay within the range of uncertainty of the measurements. The R^2 obtained is 0.987.

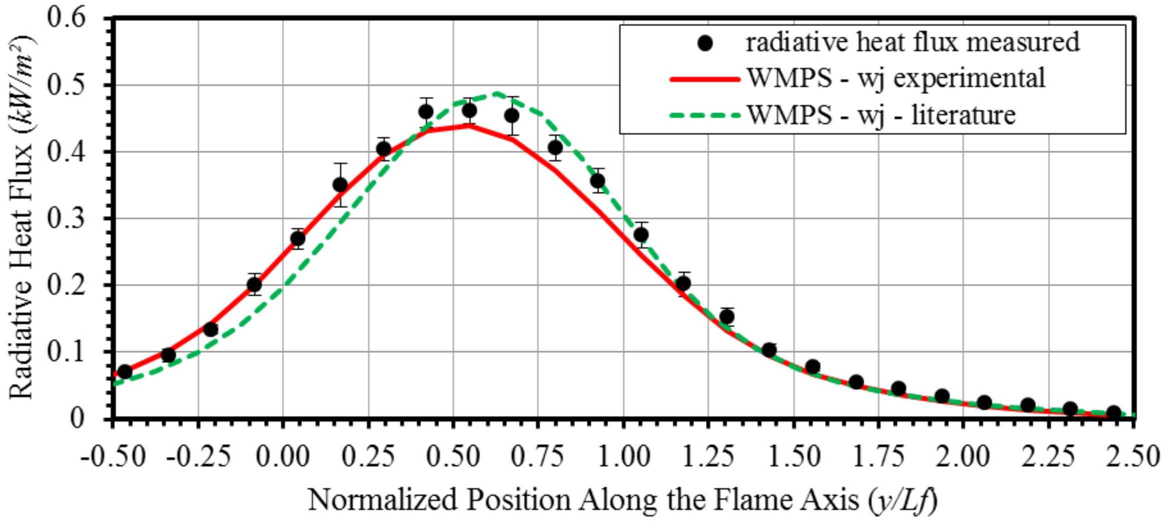

Figure 5. Distribution of the measured radiative heat flux (black circles) compared to the fluxes obtained with the WMPS model using the experimental weighting factors (continuous red line) and the weighting factors from Hankinson and Lowesmith (2012) (dashed green line) for the flame 3.00-0.00

Figure 6 presents the comparison of results for the remaining flames. The results obtained are similar to those presented for flame 3.00-0.00. The differences between the fluxes measured for flames 3.00-0.75 and 3.00-2.00 (constant heat power flames) are due basically to the reduction in the radiative heat fraction with the increase in CO_2 dilution. The differences between the flames 2.40-0.60 and 1.80-1.20 are due also to the increase of the ratio R/L_f, since L_f is reduced with the increase in dilution in the constant flow rate flames while R is kept constant.

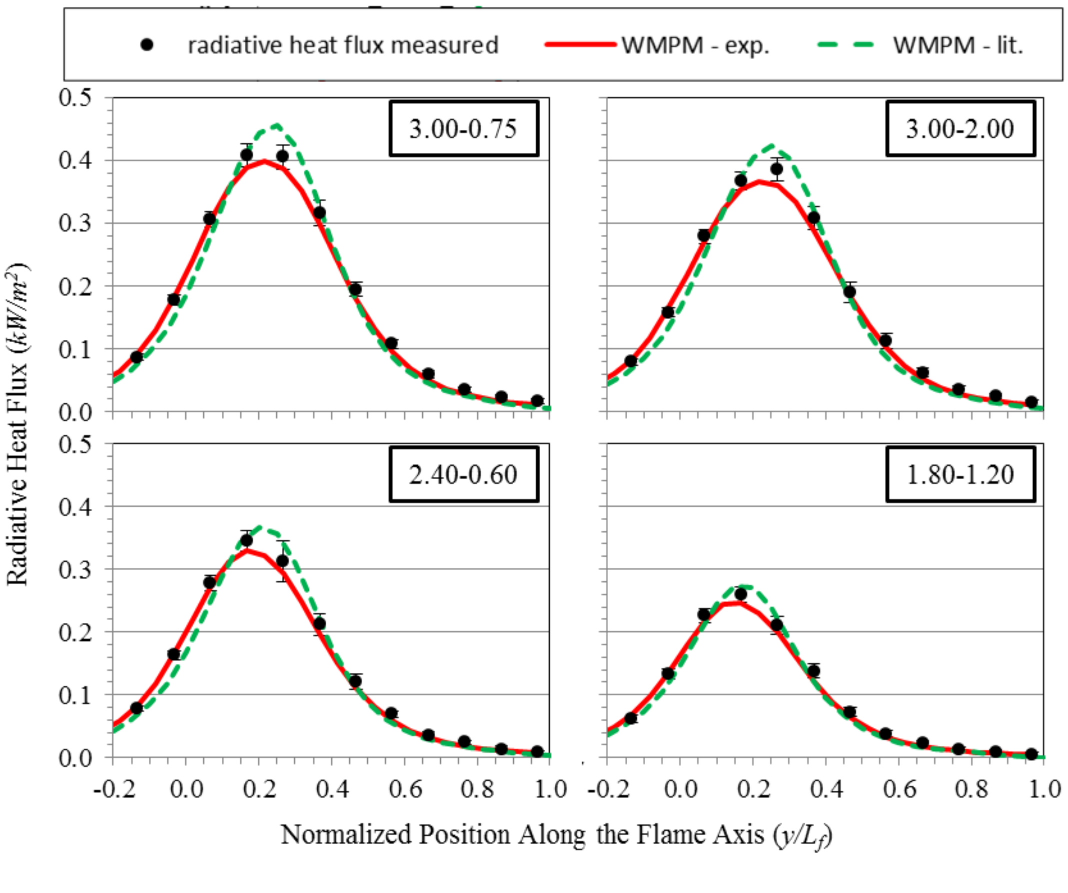

Figure 6. Distribution of the measured radiative heat flux (black circles) compared to the fluxes obtained with the WMPS model using the experimental weighting factors (continuous red line) and the weighting factors from Hankinson and Lowesmith (2012) (dashed green line) for the remaining flames

5. CONCLUSION

The addition of inert gas to the fuel reduces the visible flame length for flames with the same flow rate while flames with constant heat power show similar visible flame length for all dilutions. It is observed also the inhibition of soot formation evidenced by the reduction in the yellow luminosity of the flame and the increase in the soot free length fraction. It is observed also that the radiant fraction is reduced with the increase in CO_2 dilution, which can be related with the inhibition of soot formation and the reduction of the flame temperature.

The distribution of the weighting factors obtained is different of the presented in the literature and produces results with slightly better accordance with the radiative heat fluxes measured along the flame axis. It is also observed that the dilution do not affect significantly the distribution of weighting factors for the fuel and dilutions studied.

6. ACKNOWLEDGEMENTS

Authors thank CAPES and PETROBRAS - Petróleo Brasileiro S.A. for the financial support.

7. REFERENCES

ANSI/API 521 STANDARD, 2008. “Pressure-relieving and depressuring systems”. *American Petroleum Institute*, Washington, D. C., p.196.

Becker, H. A.; Liang, D., 1982. “Total emission of soot and thermal radiation by free turbulent diffusion flames”, *Combustion and Flame*, vol. 44, p. 305-318.

GASNET, 2013. “Gás Natural” 12 Jan. 2015 <http://www.gasnet.com.br/gasnatural/gas_completo.asp#gas12>.

Hankinson, G. and Lowesmith, B. J., 2012. “A consideration of methods of determining the radiative characteristics of jet fires”. *Combustion and Flame*, vol. 159, p. 1165-1177.

Machado, I. M., 2015. *Caracterização experimental da radiação térmica emitida por chamas não pré-misturadas de metano diluído com CO_2.* Master thesis, Federal University of Rio Grande do Sul, Brazil.

Markstein, G. H., 1977. “Scaling of radiative characteristics of turbulent diffusion flames”. *Proceedings of the Combustion Institute*, V. 16, p. 1407-1419.

Mishra, D. P. and Kumar, P., 2010. “Effects of N2 gas on preheated laminar LPG jet diffusion flame”. *Energy Conversion and Management*, Vol. 51, p. 2144-2149.

Moffat, R. J., 1988. “Describing the uncertainties in experimental results”. *Experimental Thermal and Fluid Science*, V. 1, Issue 1, p.3-17.

Nathan, G. J., Kalt, P. A. M. , Alwahabi, Z. T., Dally, B. B., Medwell, P. R. and Chan, Q. N., 2012. “Recent advances in the measurement of strongly radiating, turbulent reacting flows”. *Progress in Energy and Combustion Science*, V. 38, p. 41–61.

Sivathanu, Y. R. and Gore, J. P., 1993. “Total radiative heat loss in jet flames from single point radiative flux measurements”. *Combustion and Flame*, vol. 94, p. 265-270.

Turns, S. R., Myhr, F. H., 1991. “Oxides of nitrogen emissions from turbulent jet flames: part I – fuel effects and flame radiation”. ”. *Combustion and Flame*, V. 87, p. 319-335.

Turns, S. R., Myhr, F. H., Bandaru, R. V. and Maund, E. R., 1993. “Oxides of nitrogen emissions from turbulent jet flames: part II – fuel dilution an partial premixing effects”. *Combustion and Flame*, Vol. 93, p. 255-269.

8. RESPONSIBILITY NOTICE

The authors are the only responsible for the printed material included in this paper.